Energy minimization using the classical density distribution: Application to sodium chloride clusters

Patricia Amara and John E. Straub
Department of Chemistry, Boston University, Boston, Massachusetts 02215
(Received 27 November 1995)

The adiabatic Gaussian density annealing (AGDA) optimization algorithm, based on direct integration of the classical Bloch equation is reciprocal temperature, is employed to study the structures of $(NaCl)_n$ and $(NaCl)_nNa^+$ clusters. The results of the energy minimizations are compared with simulated annealing, using molecular dynamics. We model these clusters with a rigid core potential used in previous studies. Overall, the AGDA algorithm was successful in isolating the lowest-energy minima. In contrast to the conclusion of a previous study, we find that molecular-dynamics-based simulated annealing can be quite effective at isolating low-energy minima. However, the effectiveness of the method is strongly dependent on the integration algorithm employed. The hexagonal and cubic growth forms are found to be most stable for small clusters and the fcc structure is most stable for large clusters in agreement with previous studies. The difficulty in locating the global energy minimum is explained in terms of the statistical properties of the energy landscape. [S0163-1829(96)02120-0]

I. BACKGROUND

The structure and stability of alkali halide clusters has long been the focus of study in an effort to understand crystal growth. The lowest-energy growth pattern of small alkali halide clusters is different than that for the corresponding crystal. Experimental and theoretical studies have attempted to identify the critical value of n (number of NaCl monomers) for which the cluster can be called a crystal. In the case of sodium chloride, it has been shown that small clusters have, in general, two stable packings—hexagonal and cubic—while for larger clusters ($n>20$), the fcc structure is dominant.[1] Experiments involving mass spectrometry have been successful in relating the abundance of a given cluster size with its stability.[2–4] However, experimentally it is difficult to isolate small clusters. With mass spectrometry, only charged molecules can be studied. Therefore, computer simulation studies are necessary to study the details of their structure.

In previous studies, a ''growth algorithm'' was used to identify stable structures for each cluster size.[1,5,6] In such a method, (1) the energy of the $n-1$ cluster is minimized, (2) one monomer is added in such a way that the resulting structure is close packed, and (3) this structure is minimized. This method determines stable isomers for a given cluster size, but does not locate the global minimum exclusively. This is a difficult optimization problem, since (1) a given cluster size will have a number of stable structures that are close in energy, (2) the global minimum is often less compact than some low-lying local minima, and (3) several potentials have been used to model sodium chloride clusters and for some clusters the identity of the most stable structures can be model dependent.[5]

Simulated annealing using molecular dynamics or Monte Carlo has become the most standard optimization method. However, when there are many energy scales, the system must be slowly annealed over a broad range of temperature. This makes a simulated annealing calculation tedious as the system size increases.[6] To avoid this problem, several methods have been developed which combine the idea of simulated annealing with potential smoothing.[7–9] Potential-energy smoothing involves coarse graining over length scales on the potential hypersurface, which range from separations between local minima to distances between larger basins of attraction. The effect is to generate a coarse-grained potential hypersurface with raised minima and lowered barriers. This can allow the system to be annealed more rapidly. The most popular smoothing transform is a Gaussian integral transform, but a number of smoothing transforms, tailored to a given functional form of the potential, have also been quite successful.[10] In addition to integral transforms of the potential, $V(\mathbf{r})$, there has been progress in developing optimization algorithms based on coarse graining the Boltzmann probability density, $\exp(-\beta V(\mathbf{r}))$.[11] Such methods have the advantage of eliminating singularities in the surface, due to divergences in the core potentials. Nevertheless, all dynamical annealing algorithms must employ a cooling schedule, which is typically far from optimal.

A different form of simulated annealing which eliminates the problematic cooling schedule has recently been proposed.[9] In this method, an approximate representation of the classical density distribution is directly integrated in reciprocal temperature according to the classical Bloch equation $[d\rho_{eq}/d\beta=-(H-\langle H\rangle)\rho_{eq}]$. In this method, there is no real time dynamics—the approximate density distribution is integrated from a delocalized form ($\beta=0$) to the asymptotic low-temperature form, where the equilibrium distribution is localized in the lowest-energy minimum ($\beta=\infty$). The special case when the density distribution is approximated using a Gaussian basis is referred to as the adiabatic Gaussian density annealing (AGDA) algorithm. This method is the $\hbar=0$ limit of quantum-mechanical dynamics in Euclidean (imaginary) time and has much in common with quantum-mechanical annealing algorithms based on imaginary time methods.[12,13]

In evolving the approximate equilibrium density distribution, the center position and width of the distribution are determined by derivatives of the potential averaged over the density distribution. This amounts to a coarse graining or potential smoothing. This method can be thought of as successive minimization on an averaged potential, which is smooth at high temperature and rough at low temperatures. In fact, it has been demonstrated that smoothing transformations are closely related to thermodynamic potentials of mean force, which include a smoothing generated by an average over thermally broadened conformational distribution functions.[14,15] The AGDA algorithm has recently been successfully applied to some optimization problems, including Lennard-Jones clusters[16] and model proteins.[14]

In this paper, we apply the AGDA algorithm[9] and molecular-dynamics-based simulated annealing to identify low-energy structures of sodium chloride clusters $(NaCl)_n$ and $(NaCl)_nNa^+$. We first define the methods used in this study. We then describe a simple two-body interaction potential used to model alkali halide clusters and present the results of the minimization of these clusters. We conclude with a discussion of the results in terms of the details of the energy landscape of these clusters.

II. MINIMIZATION ALGORITHMS, POTENTIALS, AND PROTOCOLS

In this section, we present both optimization algorithms used in our study. First, we describe the algorithm for simulated annealing, using molecular dynamics (MD), and then the adiabatic Gaussian density annealing algorithm. Both methods have been previously discussed in detail.[16,14]

A. MD simulated annealing

We used simulated annealing with standard molecular dynamics based on an equation of motion derived from the Verlet algorithm for a Langevin dynamics. The random force contribution is neglected and the result is a dynamics which, on average, relaxes the system temperature exponentially in time

$$\mathbf{r}_{n+1}=\left(1+\frac{\gamma h}{2m}\right)^{-1}\left[2\mathbf{r}_n-\left(1-\frac{\gamma h}{2m}\right)\mathbf{r}_{n-1}+\frac{h^2}{m}\mathbf{F}_n\right]. \quad (1)$$

γ is a friction constant that determines the strength of the coupling to the zero-temperature heat bath and enforces an exponential cooling rate and h is the time step.

The crucial feature of this algorithm is the use of a cooling schedule that does *not* impose a rigid temperature constraint. The system is coupled to a heat bath, which allows the system temperature to fluctuate about the desired value. For the optimization of Lennard-Jones clusters, this implementation of the simulated annealing method, using MD has been shown to be far more effective than similar algorithms based on MD with a rigid temperature constraint.[17]

In a collapse or condensation transition, with an associated ''latent heat,'' the excess kinetic energy, which raises the temperature, is used to further anneal the system. The effect is to spend more time in the annealing run when the system is descending the potential hypersurface most rapidly. This is also a feature of an annealing cooling schedule based on constant ''thermodynamic speed,'' where the cooling rate is inversely proportional to the heat capacity.[9,18] The advantage of using Eq. (1) is that it requires no prior knowledge of the heat capacity.

B. Adiabatic Gaussian density annealing

In the AGDA algorithm, simulated annealing is performed directly in temperature rather than in real time as for molecular dynamics. The evolution *in temperature* of the equilibrium density distribution $\hat{\rho}(\mathbf{r},\beta)$ is defined by the classical Bloch equation,

$$\partial\rho_{\rm eq}/\partial\beta=-(H-\langle H\rangle)\rho_{\rm eq}, \quad (2)$$

where H is the classical Hamiltonian and $\langle\ \rangle$ indicates an average over the density distribution. This is the classical analog of imaginary time quantum dynamics.[9,12] The goal is to approximately solve Eq. (2) for the low temperature $\rho_{\rm eq}$ from an initial high-temperature distribution.

The system is first represented by a classical density distribution, where the density for each particle is approximated by a Gaussian packet of the form

$$\hat{\rho}(\mathbf{r},\beta)=(2\pi M_2)^{-d/2}\exp\left[-\frac{d}{2M_2}(\mathbf{r}-\mathbf{r}_0)^2\right]. \quad (3)$$

The many-body density distribution is then approximated by a Hartree product of the single-particle densities,

$$\hat{\rho}(\mathbf{r}^N,\beta)=\prod_{k=1}^{N}\hat{\rho}_k(\mathbf{r}_k,\beta). \quad (4)$$

The evolution *in temperature* of the centers and widths for each Gaussian packet is then followed, using the variationally optimal equations of motion,

$$\frac{d\mathbf{r}_0}{d\beta}=-\frac{1}{d}M_2\nabla_{r_0}\langle V\rangle, \quad (5)$$

$$\frac{dM_2}{d\beta}=-\frac{1}{d^2}M_2^2\nabla_{r_0}^2\langle V\rangle. \quad (6)$$

Initially, the widths of each packet are set to be large compared with the physical size of the cluster, so that the density distribution approximates the high-temperature distribution $\hat{\rho}(\mathbf{r},\beta=0)=$const. Integration of the distribution follows three steps. (1) The center of the distribution is minimized on the effective smoothed potential surface to bring $\hat{\rho}(\mathbf{r},\beta)$ to an ''equilibrium'' position.[16] This is equivalent to a steepest-descent minimization on the averaged potential,

$$\frac{d\mathbf{r}_0}{d\beta}=-\nabla_{r_0}\langle V\rangle, \quad (7)$$

(2) Equation (6) for the widths is integrated. (3) Return to (1). the first stage was accomplished using the conjugate gradient algorithm. The integrator used to integrate the equation of motion for the widths was the fourth-order Runge-Kutte algorithm. This version of the AGDA algorithm has provided good results for systems including Lennard-Jones clusters,[9] water clusters,[16] and a model protein.[14]

C. Alkali halide interaction potential

Alkali halide clusters have been commonly studied, using a two-body interaction potential. We chose to use the rigid core model,[1] which is composed of a long-range Coulomb interaction and a short-range repulsive Born-Mayer interaction,

$$V(r_{ij})=\frac{q_i q_j}{r_{ij}}+A\,\exp\left[-\frac{r_{ij}}{\rho}\right]. \tag{8}$$

There are only two parameters $A=1.47\times10^{-9}$ erg and $\rho=0.328$ Å (Refs. 19 and 20). This potential does not take into account charge-dipole and dipole-dipole interactions. Each particle is taken to be a rigid ion and the Na^+ and Cl^- ions are modeled with identical radii and opposite charges. This simple model, independent of the cluster size, has proved to give very good results in modeling the basic properties of $(NaCl)_n$ and $(NaCl)_nNa^+$ clusters.[1,20]

To apply the AGDA algorithm, we need to evaluate the expression for the averaged potential $\langle V\rangle$ and its derivatives. The potential being pairwise, we can evaluate the effective potential required in Eqs. (5) and (6) defined as

$$\langle V\rangle_{ij}=\int d\mathbf{r}_i\int d\mathbf{r}_j\rho_i(\mathbf{r}_i)\rho_j(\mathbf{r}_j)V(|\mathbf{r}_i-\mathbf{r}_j|), \tag{9}$$

where $\rho_i(\mathbf{r}_i)$ and $\rho_j(\mathbf{r}_j)$ are the density distributions for the ith and jth sites. The details of the derivation of $\langle V\rangle$ and its first and second derivatives are given in the Appendix.

III. RESULTS AND ANALYSIS

We applied the AGDA algorithm and molecular-dynamics simulated annealing to two different types of clusters—neutral $(NaCl)_n$ and positively charged $(NaCl)_nNa^+$. For each cluster size, we took 100 random starting configurations. In the AGDA runs, the initial width for each packet was taken to be between 50 $Å^2$ and 200 $Å^2$, depending on the cluster size. In the MD simulated annealing, the initial temperature was set to 1500 K and the friction constant determining the coupling to the heat bath was set to $\gamma=0.61$ ps^{-1}. This latter rate was chosen so that the annealing timings of both minimization methods were comparable. For both methods, a confining potential of the form $V_{\rm conf}=(\kappa/2)\Sigma_i(\mathbf{r}_i-\mathbf{r}_{\rm com})^2$ was used to avoid the explosion of the clusters during the simulation. The energies are given in eV and the lengths are given in Å.

A. Neutral $(NaCl)_n$ clusters

The global optimization results for $(NaCl)_n$ clusters are reported in Fig. 1. Overall the AGDA method was more efficient than the MD simulated annealing in finding the lowest-lying minimum. However, the global minimum was isolated for every cluster, using either method with the exception of cluster $(NaCl)_{10}$. Clusters with $n=4$, 6, and 9 were found to be particularly stable, as reported in other studies.[21] The density of minima obtained with MD and AGDA is given in Fig. 1. For each cluster size, the MD was trapped in a broad range of local minima, while the AGDA typically converged to a far smaller number of low-lying local minima.

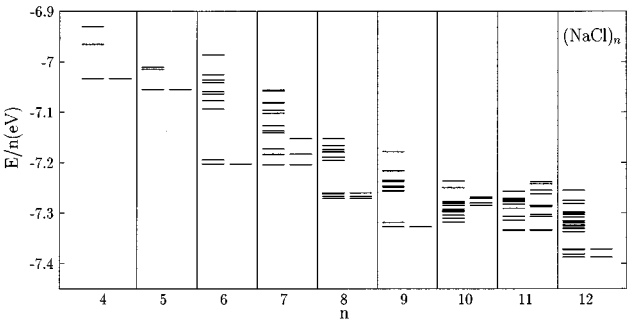

FIG. 1. The spectrum of minima obtained after both minimization methods (MD left, AGDA right) for neutral clusters $(NaCl)_n$ from $n=4$ to 12.

For the $n\geq6$ clusters, the AGDA algorithm located the global minima. The minima for these small clusters are the same as those obtained in previous studies of these systems. The MD simulated annealing typically provided average results and a particularly poor result for the tetramer $n=4$. The tetramer has been widely studied and found to have two minima very close in energy. The structure of the lowest minimum is a cube and the first local minimum is an eight-atom ring. It was reported[22] that below 500 K, the cubic configuration is favored over the ring. This result indicates that the choice of initial temperature (or in the AGDA, the choice of the initial distribution width) is an important factor in the cluster minimization. As we increased the starting temperature of the MD annealing run, there was an increased preference for the ring structure, as opposed to the lowest-energy cubic structure. On the other hand, in the case of the AGDA, as the initial value of the width of the packets was increased, the cubic configuration was favored over the ring. This can be explained by our choice for the boundary potential, which is crucial for the AGDA method.[14] When the M_2 is large (β near 0), the intermolecular potential is smoothed and the boundary potential becomes a significant part of the total potential energy. The potential that we used confines the particles to the center-of-mass, which makes the cubic configuration more likely to occur, since it is a more compact structure. As a result, our choice of boundary potential caused some problems for the optimization of larger clusters for which the global minimum is not the most compact state.

For $n>6$ clusters, the AGDA method did well in consistently identifying low-lying minima. Figure 2(a) shows the gap between the energy of the first two local minima and the global minimum for the different cluster sizes. As the cluster size increases, the energy gap is relatively smaller, which makes it difficult to locate the global minimum. We have noticed previously, in the case of a model protein, that a significant gap between the lowest minimum and the next lowest local minimum was strongly correlated with the success of the AGDA method.[14] Clusters $n=8$, 10, and 11 have many minima close in energy. Figure 2(b) compares the compactness of the minima and it shows that $(NaCl)_n$ clusters have local minima that are more compact than the global minimum. In that case, the AGDA will tend to locate these compact local minima, because of our choice of boundary potential. For example, the first and second excited states of the $(NaCl)_{10}$ cluster are more compact [see Fig. 2(b)] than

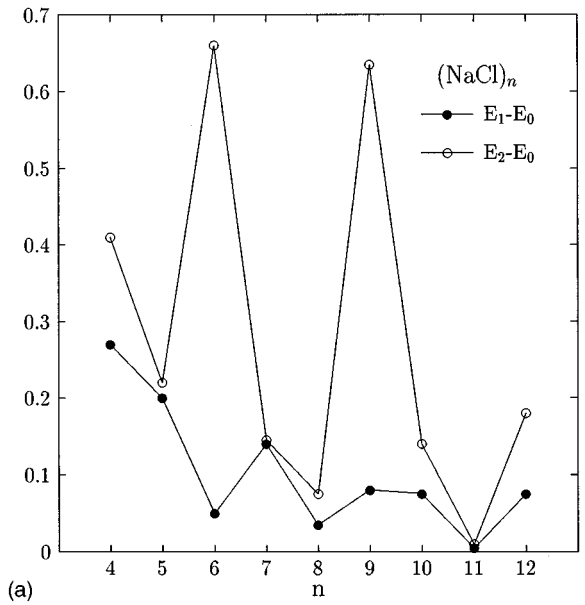

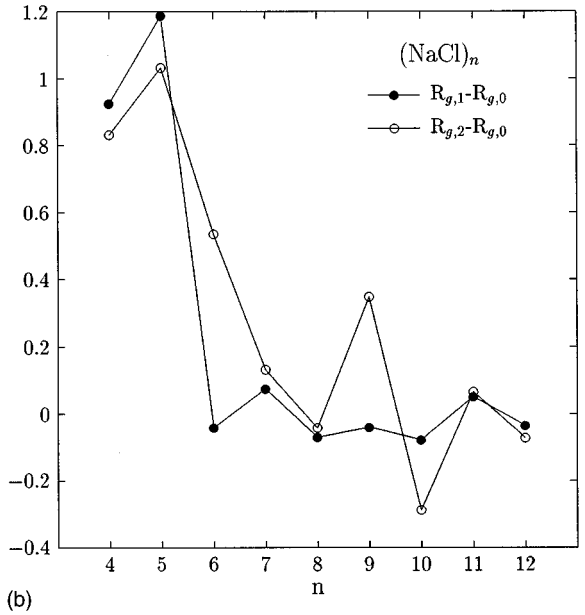

FIG. 2. (a) The energy gaps (in eV) between the global minimum and the first excited state (E_1-E_0) and the second excited state (E_2-E_0) are plotted as a function of the cluster size for $(\mathrm{NaCl})_n$. (b) The differences in radius of gyration (in Å) between the global minimum and the first excited state $(R_{g,1}-R_{g,0})$ and the second excited state $(R_{g,2}-R_{g,0})$ are also shown.

the lowest minimum, which explains the failure of our algorithm in isolating the lowest-energy minimum.

$(\mathrm{NaCl})_9$ is a very stable cluster, since it is built from stable six-ring units. This stability was confirmed by our minimization in which that structure was located 100% of the time. The lowest minimum found for $(\mathrm{NaCl})_{11}$ was reported by Phillips, Conover, and Bloomfield.[6] However, most of the time, the AGDA was trapped in the first local minimum, which is very stable and had been reported earlier to be the most stable structure.[5] The density of local minima for the $(\mathrm{NaCl})_{11}$ cluster is shown in Fig. 3. It was obtained by quenching 1000 configurations from a constant temperature MD trajectory generated at initial temperatures of $T=1500$ and 1000 K. The density of each minimum is weighted by the number of times it was located. In Fig. 3, we can see that several local minima are very stable with energies comparable to that of the global minimum.

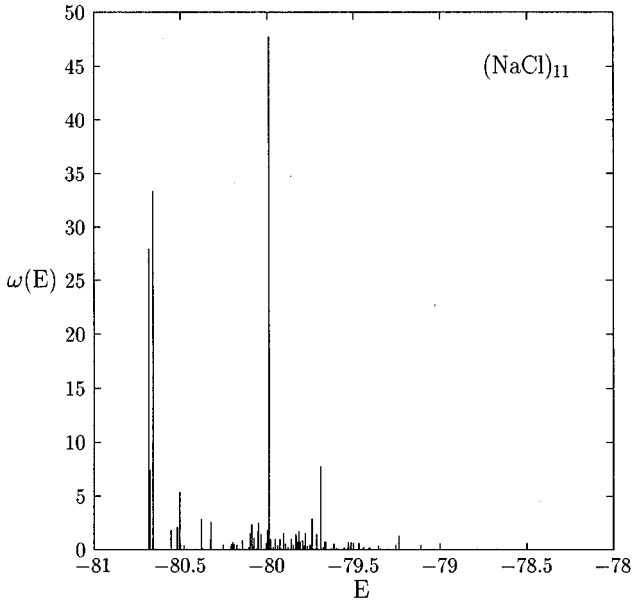

FIG. 3. The weighted density of local minima for the $(\mathrm{NaCl})_{11}$ cluster.

Since $(\mathrm{NaCl})_{12}$ contains 24 atoms—a multiple of 6 as is the case for $(\mathrm{NaCl})_6$ and $(\mathrm{NaCl})_9$—the most stable structure is four six-ring stacked. In our search of the potential hypersurface using the AGDA algorithm, we obtained a structure very similar to the $(\mathrm{NaCl})_{11}$ first local minimum. This packing was the most abundant in our minimization of $(\mathrm{NaCl})_{11}$, as shown in Fig. 4.

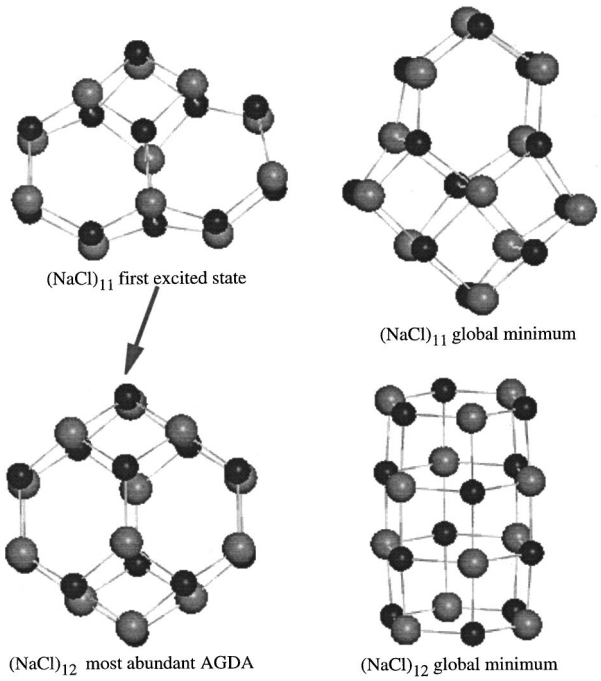

FIG. 4. Stable structures for the endecamer $(\mathrm{NaCl})_{11}$ and the dodecamer $(\mathrm{NaCl})_{12}$.

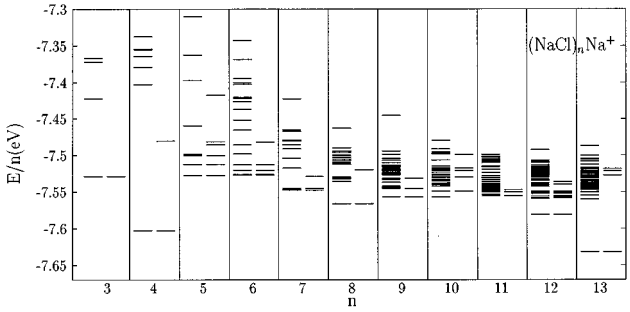

FIG. 5. The spectrum of minima obtained after both minimization methods (MD left, AGDA right) for positively charged clusters $(NaCl)_nNa^+$ from $n=3$ to 13.

For larger clusters, such as $n=13-18$, the cubic growth structures dominate. This finding is in agreement with experiments, as well as previous energy calculations.

B. Charged $(NaCl)_nNa^+$ clusters

Charged clusters are a harder optimization problem than are neutral ones. For all cluster sizes, there are many low-energy stable structures. It has been shown that these structures are also more strongly model dependent than are the neutral clusters.[5] The results of energy optimization for these clusters are reported in Fig. 5. Both the AGDA and MD simulated annealing algorithms were successful in locating the global energy minimum. An exception is the lowest-energy minimum for $n=10$, which was never located with our method. The density of states for this cluster size in Fig. 6 shows a high density of local minima with large weights that are close in energy. These large statistical weights derived from energy minimization are correlated with a large density of states for the corresponding minimum implying a large basin of attraction. These states are expected to have a lower free energy and larger statistical weight. The probability of locating a minimum is well correlated with the weighted density of states.

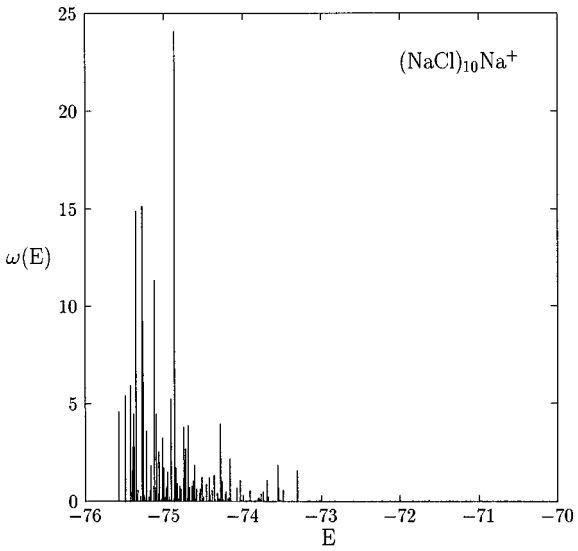

FIG. 6. The weighted density of local minima for the $(NaCl)_{10}Na^+$ cluster.

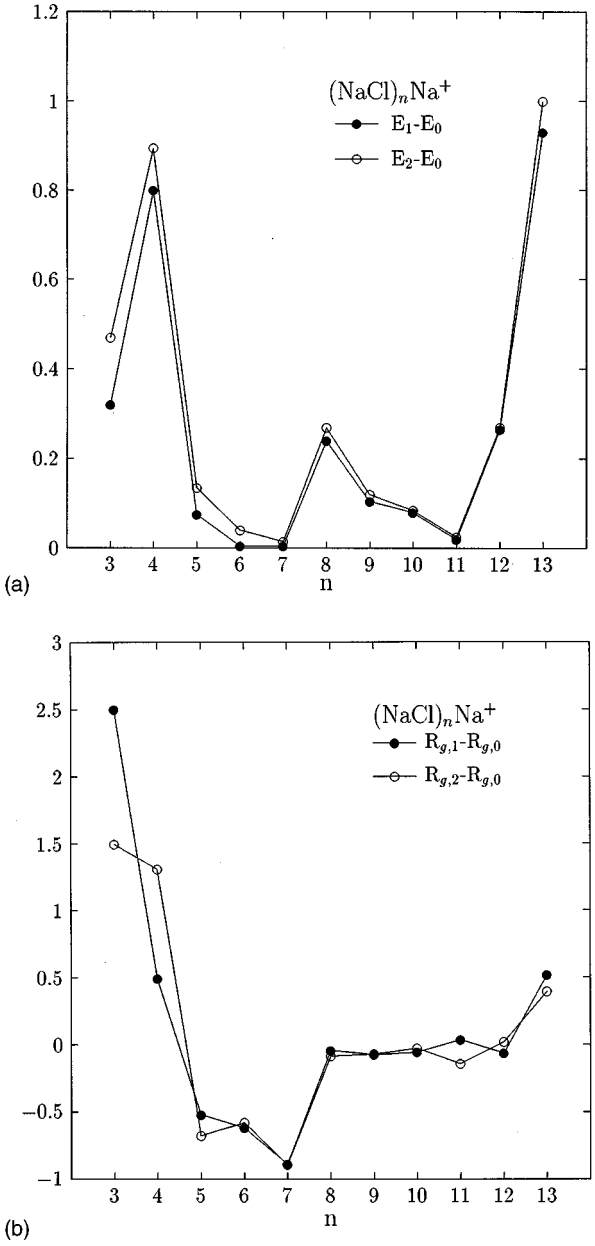

FIG. 7. (a) The energy gaps (in eV) between the global minimum and the first excited state (E_1-E_0) and the second excited state (E_2-E_0) are plotted as a function of the cluster size for $(NaCl)_nNa^+$. (b) The differences in radius of gyration (in Å) between the global minimum and the first excited state $(R_{g,1}-R_{g,0})$ and the second excited state $(R_{g,2}-R_{g,0})$ are also shown.

Clusters $n=4$, 8, and 13 were found to be particularly stable. For these three clusters, the energy splittings presented in Fig. 7(a) are relatively significant and it is rare that the system is trapped in a local minimum. In general, most of the positively charged clusters have a small energy gap and numerous compact states, as demonstrated in Fig. 7(b) for clusters $n=5-7$ and $n=9-12$. As in the case of neutral clusters, the MD simulated annealing runs are often trapped in high-lying local minima, while the AGDA algorithm tends to isolate a few low-lying minima.

The $(NaCl)_{13}Na^+$ cluster has a relatively high binding energy, due to its high symmetry $(3\times3\times3)$. Its global mini-

mum is a cubic portion of an fcc lattice. This high stability was confirmed by our study. The cubic growth structure is found to be prevalent for $n \geqslant 13$ as for the neutral clusters.

IV. CONCLUSIONS

We find that both the AGDA and MD simulated annealing algorithms are successful in isolating the global minimum of alkali halide clusters. We find that clusters that were known to be thermodynamically very stable with a large energy gap between the ground and first excited-state minima tend to be relatively easy optimization problems. Clusters, which have many low-lying minima that are at the bottom of large basins of attraction, represent hard optimization problems. For such clusters, runs are often trapped in low-lying local minima. There is a strong correlation between the energy gap and the success of either algorithm. In cases where local minima were more compact than the global energy minimum [see the $(NaCl)_{10}$ cluster], the AGDA algorithm applied with a spherically symmetric boundary potential tended to isolate low-lying local minima.

In their study, Phillips and co-workers[6] argued that simulated annealing using molecular dynamics failed for alkali halide clusters, because of the character of the energy landscape (a point discussed in detail in this study). Most of these clusters have many low-lying minima, which demands that the MD annealing be done very slowly. The method they used[23] is a Monte Carlo (MC) technique, combined with a slow cooling schedule that gave good results for a series of Lennard-Jones clusters. Phillips found that, for the alkali halide clusters, the cooling time became too large as the number of atoms increased. However, in our study, we employed an annealing protocol based on a modified Langevin dynamics. This algorithm led to excellent results, as it did for the Lennard-Jones clusters.[17] The conclusion is that the effectiveness of simulated annealing is strongly dependent on the search algorithm (MC or MD) for cases where a nonoptimal cooling schedule is employed. The MD simulated annealing algorithm employed in this study appears to be significantly more effective than any simulated annealing algorithms, that we are aware of, which are used in the study of molecular optimization problems.

ACKNOWLEDGMENTS

J.E.S. gratefully acknowledges the Alfred P. Sloan Foundation for support and the National Science Foundation (CHE-9306375) for support and computational resources at the Pittsburgh Supercomputing Center (CHE-930040P).

APPENDIX: DERIVATION OF $\langle V \rangle$ AND ITS FIRST AND SECOND DERIVATIVES

Here, we state the coarse-grained effective potential and its derivatives for the Born-Mayer potential $V_{\mathrm{BM}} = \exp[-r_{ij}/\rho]$ and the spherical Gaussian density distribution.

$$\langle V_{\mathrm{BM}} \rangle = \left(1 - \frac{1}{2\beta r_{ij}\rho}\right) \frac{\mathrm{erfc}(x_m)}{2} \exp\left[-\frac{r_{ij}}{\rho} + \frac{1}{4\beta\rho^2}\right] + \left(1 + \frac{1}{2\beta r_{ij}\rho}\right) \frac{\mathrm{erfc}(x_p)}{2} \exp\left[\frac{r_{ij}}{\rho} + \frac{1}{4\beta\rho^2}\right], \tag{A1}$$

$$\nabla_{r_{0,i}} \langle V_{\mathrm{BM}} \rangle = -\frac{1}{2r_{ij}\rho}(\mathbf{r}_i - \mathbf{r}_j) \left\{ -\frac{2}{\beta r_{ij}} \left(\frac{\beta}{\pi}\right)^{1/2} \exp[-\beta r_{ij}^2] + \mathrm{erfc}(x_m) \exp\left[-\frac{r_{ij}}{\rho} + \frac{1}{4\beta\rho^2}\right] \left[\frac{1 + r_{ij}/\rho}{2\beta r_{ij}^2} - 1\right] + \mathrm{erfc}(x_p) \exp\left[\frac{r_{ij}}{\rho} + \frac{1}{4\beta\rho^2}\right] \left[\frac{-1 + r_{ij}/\rho}{2\beta r_{ij}^2} + 1\right] \right\}, \tag{A2}$$

$$\nabla_{r_{0,i}}^2 \langle V_{\mathrm{BM}} \rangle = \frac{1}{r_{ij}\rho} \left\{ \mathrm{erfc}(x_m) \exp\left[-\frac{r_{ij}}{\rho} + \frac{1}{4\beta\rho^2}\right] \times \left(-1 - \frac{1}{4\beta\rho^2} + \frac{r_{ij}}{2\rho}\right) + \mathrm{erfc}(x_p) \times \exp\left[\frac{r_{ij}}{\rho} + \frac{1}{4\beta\rho^2}\right] \left(1 + \frac{1}{4\beta\rho^2} + \frac{r_{ij}}{2\rho}\right) \right\}, \tag{A3}$$

where $\beta = d/[M_2(i) + M_2(j)]$, $x_m = -\sqrt{\beta} r_{ij} + 1/(2\sqrt{\beta}\rho)$, and $x_p = \sqrt{\beta} r_{ij} + 1/(2\sqrt{\beta}\rho)$.

For the Coulomb interaction, we need to average the potential of the form $V_c = 1/r_{ij}$. The average potential and its derivatives are

$$\langle V_c \rangle = \frac{1}{r_{ij}} \mathrm{erf}(r_{ij}\sqrt{\beta}), \tag{A4}$$

$$\nabla_{r_{0,i}} \langle V_c \rangle = (\mathbf{r}_i - \mathbf{r}_j) \left[-\frac{\mathrm{erf}(r_{ij}\sqrt{\beta})}{r_{ij}^3} + \frac{2\sqrt{\beta}}{r_{ij}^2\sqrt{\pi}} \exp[-\beta r_{ij}^2] \right], \tag{A5}$$

$$\nabla_{r_{0,i}}^2 \langle V_c \rangle = -4\beta\sqrt{\beta/\pi} \exp[-\beta r_{ij}^2]. \tag{A6}$$

For the confining potential of the form $V_{\mathrm{conf}} = (\kappa/2)\Sigma_i (\mathbf{r}_i - \mathbf{r}_{\mathrm{com}})^2$, the effective potential and its derivatives are

$$\langle V_{\mathrm{conf}} \rangle = \frac{\kappa}{2} \sum_i \left[(\mathbf{r}_{0,i} - \mathbf{r}_{\mathrm{com}})^2 + M_2(i) \right], \tag{A7}$$

$$\nabla_{r_{0,i}} \langle V_{\mathrm{conf}} \rangle = \kappa (\mathbf{r}_{0,i} - \mathbf{r}_{\mathrm{com}}), \tag{A8}$$

$$\nabla_{r_{0,i}}^2 \langle V_{\mathrm{conf}} \rangle = \kappa d. \tag{A9}$$

We used a small value for κ to bias our search in favor of the set of compact, low-energy minima.

[1] T. P. Martin, Phys. Rep. **95**, 167 (1983).
[2] J. E. Campana, T. M. Barlak, R. J. Colton, J. J. DeCorpo, J. R. Wyatt, and B. I. Dunlap, Phys. Rev. Lett. **47**, 1046 (1981).
[3] R. Pflaum, P. Pfau, K. Sattler, and E. Recknagel, Surf. Sci. **156**, 165 (1984).
[4] Y. J. Twu, C. W. S. Conover, Y. A. Yang, and L. A. Bloomfield, Phys. Rev. B **42**, 5306 (1990).
[5] J. Diefenbach and T. P. Martin, J. Chem. Phys. **83**, 4585 (1985).
[6] N. G. Phillips, C. W. S. Conover, and L. A. Bloomfield, J. Chem. Phys. **94**, 4980 (1991).
[7] L. Piela, J. Kostrowicki, and H. A. Scheraga, J. Phys. Chem. **93**, 3339 (1989); J. Kostrowicki, L. Piela, B. J. Cherayil, and H. A. Scheraga, *ibid.* **95**, 4113 (1991); R. J. Wawak, M. M. Wimmer, and H. A. Scheraga, *ibid.* **96**, 5138 (1992); J. Kostrowicki and H. A. Scheraga, *ibid.* **96**, 7442 (1992).
[8] J. Ma, D. Hsu, and J. E. Straub, J. Chem. Phys. **99**, 4024 (1993).
[9] J. Ma and J. E. Straub, J. Chem. Phys. **101**, 533 (1994).
[10] J. E. Straub, in *New Developments in Theoretical Studies of Proteins*, edited by R. Elber (World Scientific, Singapore, 1996).
[11] D. Shalloway, in *Recent Advances in Global Optimization*, edited by A. Floudas and P. M. Pardalos (Princeton University Press, Princeton, 1992), p. 433.
[12] P. Amara, D. Hsu, and J. E. Straub, J. Phys. Chem. **97**, 6715 (1993).
[13] A. B. Finnila, M. A. Gomez, C. Sebenik, C. Stenson, and J. D. Doll, Chem. Phys. Lett. **219**, 343 (1994).
[14] P. Amara and J. E. Straub, J. Chem. Phys. **99**, 14 840 (1995).
[15] J. E. Straub, P. Amara, and J. Ma, J. Chem. Phys. **103**, 1574 (1995).
[16] C. Tsoo and C. L. Brooks III, J. Chem. Phys. **101**, 6405 (1994).
[17] J. Ma and J. E. Straub, J. Chem. Phys. **103**, 9113 (1995).
[18] P. Salamon, J. D. Nulton, J. R. Harland, J. Pedersen, G. Ruppeiner, and L. Liao, Comput. Phys. Commun. **49**, 423 (1988).
[19] M. Born and K. Huang, *Dynamical Theory of Crystal Lattices* (Oxford, London, 1954), p. 26.
[20] T. P. Martin, J. Chem. Phys. **67**, 5207 (1977).
[21] A. Ayuela, J. M. López, J. A. Alonso, and V. Luana, An. Fis. **90**, 191 (1994).
[22] T. P. Martin, J. Chem. Phys. **72**, 3506 (1980).
[23] L. T. Wille, Chem. Phys. Lett. **133**, 405 (1987).